IEEE Photonics Journal
An IEEE Photonics Society Publication

Demonstration of Laser-Fabricated DLSPPW at Telecom Wavelength

Volume 2, Number 4, August 2010

Andreas Seidel
Carsten Reinhardt
Tobias Holmgaard
Wei Cheng
Tiberiu Rosenzveig
Kristjan Leosson
Sergey I. Bozhevolnyi
Boris N. Chichkov

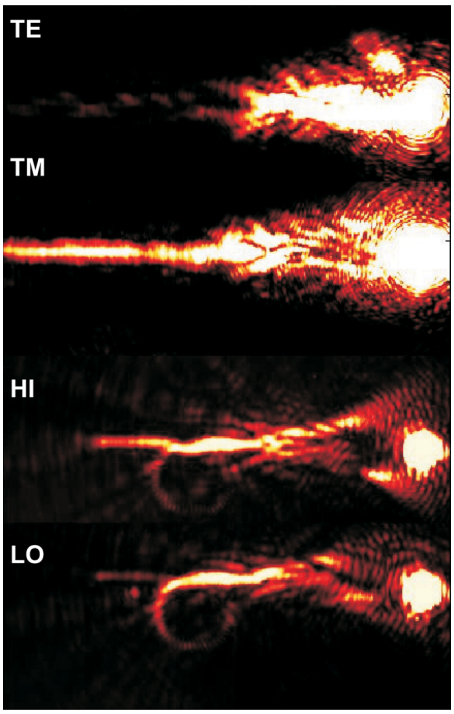

DOI: 10.1109/JPHOT.2010.2056490
1943-0655/$26.00 ©2010 IEEE

IEEE photonics SOCIETY
IEEE

Demonstration of Laser-Fabricated DLSPPW at Telecom Wavelength

Andreas Seidel,[1] Carsten Reinhardt,[1] Tobias Holmgaard,[2] Wei Cheng,[1] Tiberiu Rosenzveig,[3] Kristjan Leosson,[3] Sergey I. Bozhevolnyi,[4] and Boris N. Chichkov[1]

[1]Laser Zentrum Hannover e.V., 30419 Hannover, Germany
[2]Department of Physics and Nanotechnology, Aalborg University, 9220 Aalborg Øst, Denmark
[3]Science Institute, University of Iceland, 107 Reykjavik, Iceland
[4]Institute of Sensors, Signals, and Electrotechnics, University of Southern Denmark, 5230 Odense M, Denmark

DOI: 10.1109/JPHOT.2010.2056490
1943-0655/$26.00 ©2010 IEEE

Manuscript received June 1, 2010; revised June 23, 2010; accepted June 23, 2010. Date of publication June 29, 2010; date of current version July 19, 2010. This work was supported by the PLASMOCOM project under Grant EC FP6 IST 034754 STREP, COST Action MP 0803, and the Center for Quantum Engineering and Space-Time Research (QUEST). Corresponding author: A. Seidel (e-mail: a.seidel@lzh.de).

Abstract: We investigate dielectric-loaded surface plasmon-polariton waveguides (DLSPPWs) fabricated by two-photon polymerization direct laser writing and nanoimprinting at the telecom wavelength of 1550 nm. We examine several types of structures such as lines and bends as individual plasmonic components. Racetrack resonators are presented as a potential application of this technology. These plasmonic components can be investigated at 1550-nm wavelength by leakage radiation microscopy using an InGaAs camera. The experimentally observed behavior of these components in a leakage radiation microscope matches the theoretical expectations. The results demonstrate the practical feasibility of laser-fabricated DLSPPW components at telecom wavelength.

Index Terms: Plasmonics, DLSPPW, two-photon polymerization.

1. Introduction

Future increases of speed and efficiency in the area of information technology require a shift from electronic to photonic components and their miniaturization. Such a route of technological development demands new materials with the capability to guide optical signals at dimensions shorter than the wavelength, below the diffraction limit. Within the field of nanophotonics, plasmonics, and, in particular, plasmonic waveguides offer such a route.

Surface plasmon-polaritons (SPPs) are collective oscillations of surface electrons in a metal coupled to light at the metal–dielectric interface [1], along which they can propagate and along which they are highly confined [2]. Components utilizing propagating SPPs have been proposed for performing a variety of functions, such as highly sensitive sensing [3], but are particularly promising in the area of information technology to provide a link between electronics and integrated optics [4], [5]. Several technologies have been proposed for plasmonic waveguides, including metal strips embedded in a dielectric also known as long-range plasmons [6], the opposite configuration—dielectric stripes embedded in metal [7], and nanowires [8]. Another approach is that of dielectric-loaded surface plasmon-polariton waveguides (DLSPPWs), which is generating growing interest and attention [9]–[15].

We present DLSPPW structures fabricated by two-photon polymerization (2PP) direct laser writing technology and nanoimprinting using molds from masters made by the aforementioned

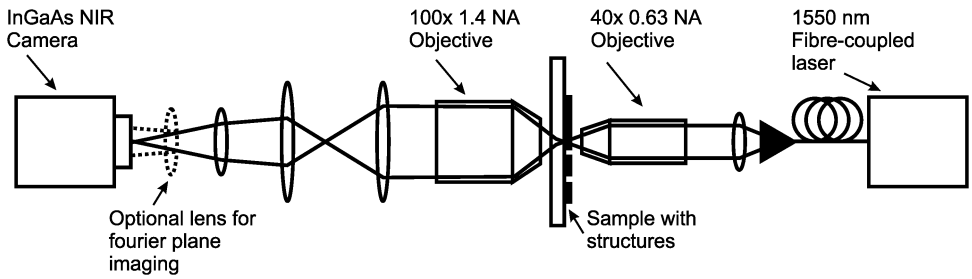

Fig. 1. Schematic image of the leakage radiation microscopy setup. An additional lens can be inserted just in front of the camera for Fourier plane imaging.

method. The structures are analyzed by leakage radiation microscopy at the 1550-nm telecommunications wavelength.

Two-photon polymerization has already been shown to be a highly flexible, versatile, and efficient tool in making DLSPPW structures [16]–[18]. The greatest advantage of this technique compared to, for example, UV mask lithography, is the fact that it is suitable as a rapid prototyping technique of DLSPPW structures, where new designs can be rapidly and cheaply produced. Nanoimprinting large numbers of structures in parallel has been used for the fabrication of plasmonic waveguides in general [4] and has also been demonstrated to work for DLSPPW structures [19].

2. Structure Fabrication

Using the 2PP method, the structures are directly written in a UV-curable photoresist on a glass substrate covered with a 50-nm gold layer. The photoresist is the spincoatable mr-NIL 6000.3 made by the company microresist in Berlin, Germany. The gold layer must be thick enough to support SPPs with reasonable propagation length, and at the same time, it must be thin enough to allow for sufficient leakage radiation to obtain useful measurement data. Fifty nanometers has proved to be the optimum thickness for fulfilling both requirements. After development, the DLSPPW structures consist of ridges of 500–600-nm width and 500-nm height. This geometry has been shown to be a single-mode plasmonic waveguide at 1550 nm [20], [21].

While the 2PP process is fast and highly flexible, it is a serial process not well adapted for mass-production of plasmonic components. Therefore, we consider it important to show that nanoimprinting (a parallel process) is also a suitable fabrication method. Here, master structures are fabricated on glass and used to make a PDMS mold, which in turn is used to imprint structures using the same photoresist as above onto a new glass substrate also covered with a 50-nm gold layer. The entire procedure is given in more detail in source [19].

3. Experimental Setup

For the characterization of the DLSPPW, leakage radiation microscopy is applied. This method has been demonstrated at visible wavelengths [19], [22]. Here, we use the same method at telecom wavelength wavelengths to demonstrate its applicability to the near-infrared regime.

As our primary light source we use a fiber laser emitting at 1550 nm. After collimation, the light is focused by a 40 $\times$ 0.63 NA objective onto the structures. To collect the leakage radiation it is necessary to use a high-NA objective due to the shallow emission angle. We use a 100 $\times$ 1.4 NA objective with oil immersion. The light is then focused onto a Hamamatsu InGaAs camera, which is highly sensitive in this spectral range. The camera is used to image both the direct image plane, as well as the Fourier plane by adding an additional lens. A schematic of the setup is shown in Fig. 1.

4. Leakage Radiation Microscopy Results and Interpretation

We show DLSPPW mode propagation on several different samples and different DLSPPW geometries. First, we will consider straight waveguides of 50–100 μm length with funnels attached on one end to aid excitation of the DLSPPW mode. The funnels have a base width of 10 μm and are

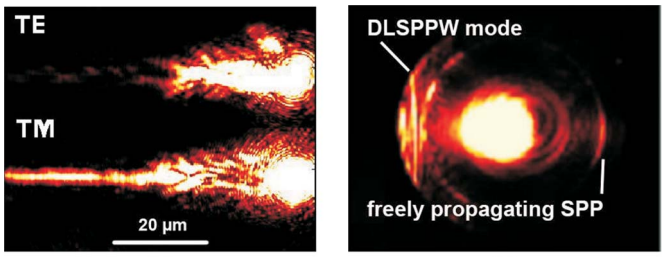

Fig. 2. Leakage radiation microscope images of a line waveguide with funnel, being excited at the funnel end by TE and TM polarized light, respectively. As can be seen in (a), the waveguide cannot support an optical TE mode but only a plasmonic TM mode. The Fourier plane image of the TM mode is shown in (b).

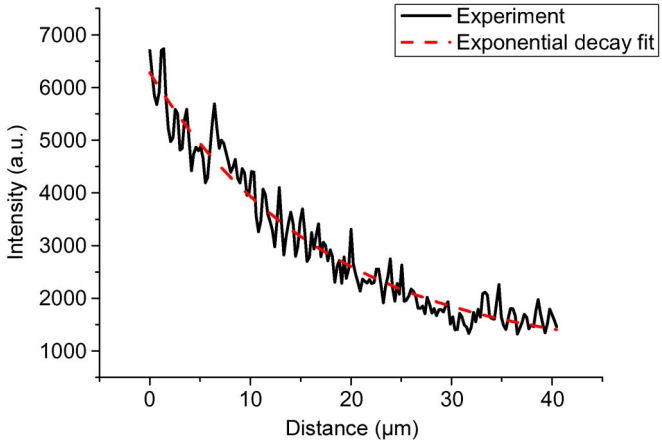

Fig. 3. Plot of the leakage radiation measured inside a line waveguide which is a direct indication of radiation intensity. An exponential fit is also shown.

25 μm long. We excite the DLSPPW mode in all our structures by focusing our laser beam on the edge of the funnel base. The resulting SPPs are viewed by leakage radiation microscopy. Fig. 2 illustrates the fact that the DLSPPW structures can only support plasmonic TM modes and not optical TE modes. While the waveguide is brightly illuminated in TM mode, showing strong evidence of leakage radiation from a plasmonic mode, it is completely dark when polarization is switched to TE. The Fourier plane image is also shown in Fig. 2. By taking into account that the innermost circle of the image corresponds to our objective's NA of 0.63, we can calculate the real part of the effective index of our DLSPPW structure simply by measuring the distance of the mode from the center of the circle. We measure an effective index of $\mathrm{Re}(n_{\mathrm{eff}}) = 1.13 \pm 0.01$. This low value is due to the refractive index $n = 1.29$ of the polymer.

The intensity of the DLSPPW mode inside the waveguide is measured using the leakage radiation, which is fitted to an exponential curve to extract the propagation length L_{prop}. That this is a reasonable method and provides a good match can be seen in Fig. 3, where such a fit curve is superimposed on the experimental results. The waveguides are clearly single mode, an improvement over the multimode waveguides published previously [14]. An analysis of the decay rate of the DLSPPW mode in several straight waveguides (line waveguides) with funnels, combined with the effective index $n_{\mathrm{eff}} = 1.13$, gives us an average propagation length of $L_{\mathrm{prop}} = 20 \pm 1$ μm. This shows some improvement compared with figures previously published using similar structures fabricated by UV mask lithography [23].

Additionally, we have a nanoimprinted version of the line waveguide. Fig. 4 shows a DLSPPW mode propagating inside a nanoimprinted line waveguide. Analysis of the mode decay rate in these

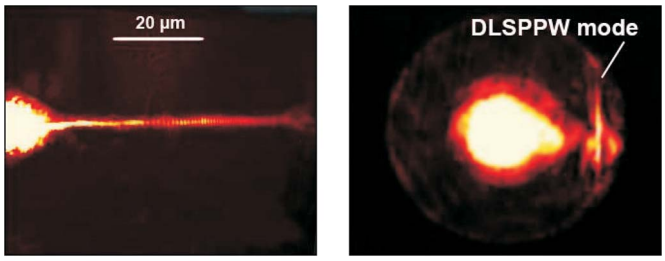

Fig. 4. (a) Leakage radiation microscopy image showing a nanoimprinted line waveguide with incoupling funnel. (b) The Fourier plane image of the same line.

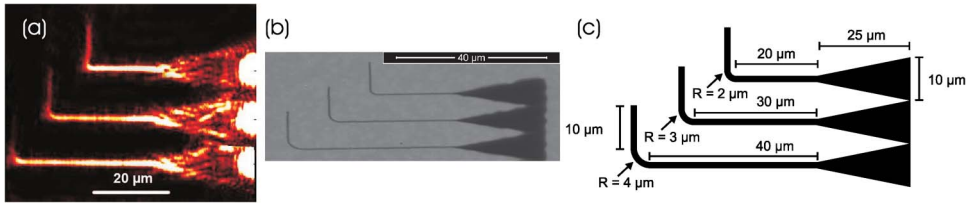

Fig. 5. (a) Leakage radiation microscope images of three bends with different curve radius. Descending from top to bottom, the curve radius is 2, 3 and 4 μm. The three images were taken separately and then merged. (b) SEM image of the structures. (c) A schematic drawing of the structures.

TABLE 1

Transmission results for bend DLSPPW structures

bend radius (μm)	transmission
2	0.17
3	0.26
4	0.31

nanoimprinted waveguides reveals an effective index $n_{\text{eff}} = 1.11$ and a propagation length of $L_{\text{prop}} = 7.6 \pm 0.3$ μm. These results are in the same range as previous results from nanoimprinted waveguides examined at 632-nm wavelength [19], but in contrast to the previous waveguides, these are single mode. There is a significant difference in the value of the propagation length when we compare the nanoimprinted and the directly written case. The explanation for this is the presence of a thin residual layer of polymer covering the sample surface in the nanoimprinted case, which leads to increased scattering, and the inclusion of dust particles in the nanoimprinting process, which leads to increased roughness and minor distortions of the structures. Both of these aspects could be improved by using more advanced equipment in a cleanroom environment.

To realize fully the potentials of DLSPPW structures for proposed miniature photonic-plasmonic hybrid circuits [24], curved waveguides are necessary. In fact, the minimal bend radius with tolerable signal losses defines the level of miniaturization that is obtainable; therefore, the investigation of bended DLSPPWs is a prerequisite for more complicated components. A series of 90° bends fabricated directly on gold by 2PP was investigated. We find that for bend radii of 2, 3 and 4 μm, the DLSPPW mode is guided through the bend, albeit with some scattering out of the waveguide. An image of the bends is shown in Fig. 5. An SEM image showing the design of the entire structure is also shown. The bend structure is designed to ease fabrication and characterization by providing a compact structure with a common baseline.

Transmission measurements were performed using the leakage radiation. The starting and ending points of the waveguide bend itself were taken as reference points for each waveguide, without regard to the incoupling waveguides. The results, which are listed in Table 1), show that

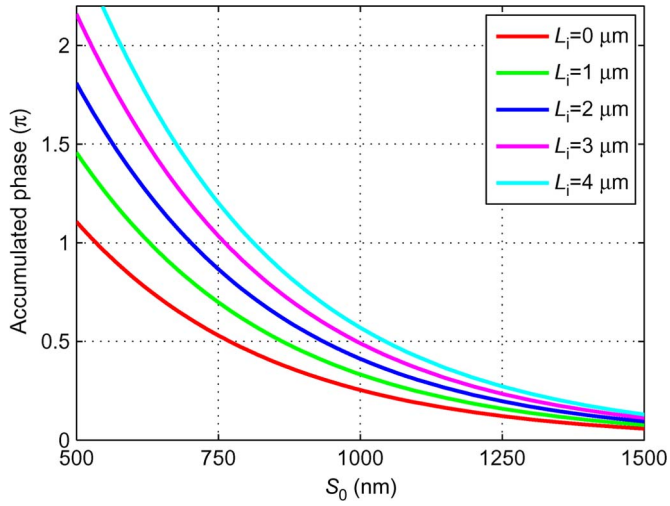

Fig. 6. EIM calculation of the accumulated phase difference ($\lambda = 1550$ nm) throughout the racetrack resonator as a function of the center-to-center separation of the (500-nm-wide and 600-nm-tall) waveguide ridges in the parallel section ($S_0 = 500$ nm corresponds to the absence of gap). The accumulated phase is plotted in units of π for different lengths of the parallel section ranging from $L_i = 0$ μm (ring resonator) to $L_i = 4$ μm. The waveguide parameters are adapted from [26].

waveguides with larger bend radii are more efficient at guiding the DLSPPW mode around a corner due to the reduction in bend scattering losses.

A more-complex DLSPPW component is a racetrack resonator. These resonators consist of a racetrack-shaped line in close proximity to a straight-line waveguide. In our investigations, the gap between racetrack and line was 500 nm. The DLSPPW mode can couple from the line waveguide in which it is launched to the racetrack resonator. Depending on wavelength or resonator length, the radiation inside the racetrack will be either in phase or out of phase with the mode in the line waveguide, which will lead to constructive or destructive interference. As such, these racetrack resonators can act as resonant filters for a variable-frequency signal. Ring-shaped DLSPPW resonators fabricated by UV lithography have already been shown to work in very similar fashion with variable laser frequency [25].

Racetrack resonators differ from ring resonators in that they have a straight interaction section which runs parallel with the waveguide, thus elongating the interaction region. This implies that one can increase the waveguide-resonator separation for a desired coupling ratio to the resonator, thus relaxing the requirements on the resolution in the fabrication. This feature is demonstrated by calculating the accumulated phase difference throughout the whole racetrack resonator (see Fig. 6), using effective index method (EIM) calculations and the supermode approach, which has previously proven accurate for describing the coupling between two adjacent DLSPPWs [26].

In plasmonic resonators, one usually requires ca. 50% coupling to the resonator [25] in order to obtain critical coupling, which translates into an accumulated phase difference of $\pi/2$. For a ring resonator, this can be achieved with a center-to-center separation of $S_0 = 770$ nm, implying a gap of only 270 nm, whereas a racetrack resonator with a parallel section of 3 μm, increases this gap to 500 nm, as shown in Fig. 6. Such an increase is in many fabrication techniques crucial in order to realize well-resolved structures, thus making the racetrack resonator a promising structure in plasmonics.

An example of racetrack resonators, fabricated directly on gold by 2PP, in operation is shown in Fig. 7, where two slightly different racetrack resonators are shown. The long waveguide (at the top in the image) shows constructive interference in the output waveguide. The difference in length of the racetrack resonators in the two pictures is 2 μm. To translate this into effective wavelengths, we must first calculate the value of the effective wavelength in the waveguide using the effective index $n_{\text{eff}} = 1.13$, which gives us $\lambda_{\text{eff}} = 1.3717$ μm. If we then divide the length difference by this value,

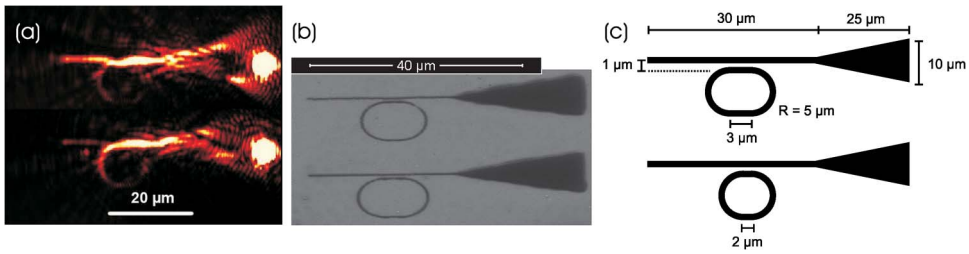

Fig. 7. (a) Leakage radiation microscope images of two racetrack resonator structures. The length difference between the two racetracks is 2 μm, which amounts to a nearly 180° phase difference, resulting in destructive interference at the waveguide output in the case of the shorter racetrack resonator. The damping is in excess of 16 dB. (b) SEM image of the structures. (c) A schematic drawing of the structures.

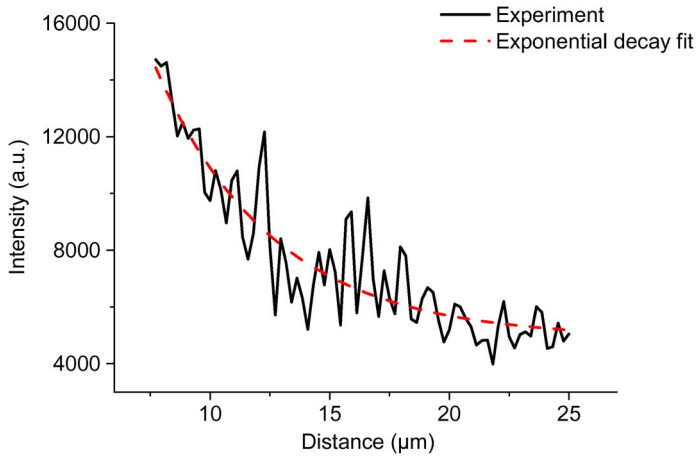

Fig. 8. Plot of the leakage radiation intensity inside the semi-circular bend of a racetrack waveguide. An exponential fit is also shown.

we get a difference of 1.46 wavelengths. Consequently, the phase change is nearly 180°, leading to an expectation of a high suppression of output in the case of the shorter resonator, which is precisely what we see in the experimental results. However, the racetrack resonator and subsequent interference is not the main cause of this result. The measured propagation length for the 5 μm semi-circular bend is $L_{\text{prop}} = 4.92 \pm 0,72$ μm, indicating some scattering out of the waveguide, which is also visible in the image. A plot of the intensity inside the bend and a superimposed exponential fit is shown in Fig. 8.

When we now consider the total length of the racetrack resonator, it becomes clear that the signal inside the racetrack becomes too weak to interfere significantly with the signal inside the line waveguide. The results stem from the fact that in the case of a 3-μm interaction length, the phase difference along this stretch is close to 2π, which means that the mode couples to the racetrack and back again. In the case of the shorter interaction length, the mode couples only to the racetrack and is diverted away. The large coupling is due to the low mode effective index of 1.13 and the corresponding low mode confinement.

5. Conclusion

In conclusion, we have demonstrated DLSPPW mode guiding by leakage radiation microscopy in laser-fabricated and nanoimprinted DLSPPW structures at the 1550-nm telecommunication wavelength. We presented DLSPPW racetrack resonators as a potential application of this technology in the form of resonant filters. The racetrack resonators show large coupling to the resonator. Due to

the low mode confinement, the coupling is much larger than anticipated, and due to the low propagation length, the fabricated structures do not operate as designed, but this can be remedied by increasing the mode effective index by using different waveguide materials in the future.

References

[1] S. A. Maier, *Plasmonics—Fundamentals and Applications*. New York: Springer-Verlag, 2007.
[2] H. Raether, *Surface Plasmons on Smooth and Rough Surfaces and on Gratings*. New York: Springer-Verlag, 1988.
[3] S. Lal, S. Link, and N. J. Halas, "Nano-optics from sensing to waveguiding," *Nat. Photon.*, vol. 1, no. 11, pp. 641–648, Nov. 2007.
[4] A. Boltasseva, "Plasmonic components fabrication via nanoimprint," *J. Opt. A, Pure Appl. Opt.*, vol. 11, no. 11, p. 114001, Sep. 2009.
[5] T. W. Ebbesen, C. Genet, and S. I. Bozhevolnyi, "Surface-plasmon circuitry," *Phys. Today*, vol. 61, no. 5, pp. 44–50, 2008.
[6] A. Degiron, P. Berini, and D. R. Smith, "Guiding light with long-range plasmons," *Opt. Photon. News*, vol. 19, no. 7, pp. 29–34, 2008.
[7] E. Verhagen, J. Dionne, L. Kuipers, H. Atwater, and A. Polman, "Near-field visualization of strongly confined surface plasmon polaritons in metal-insulator-metal waveguides," *Nano Lett.*, vol. 8, no. 9, pp. 2925–2929, Sep. 2008.
[8] K. Leosson, T. Rosenzveig, P. Hermannsson, and A. Boltasseva, "Compact plasmonic variable optical attenuator," *Opt. Express*, vol. 16, no. 20, pp. 15 546–15 552, Sep. 2008.
[9] R. Wan, F. Liu, and Y. Huang, "Ultrathin layer sensing based on hybrid coupler with short-range surface plasmon polariton and dielectric waveguide," *Opt. Lett.*, vol. 35, no. 2, pp. 244–246, Jan. 2010.
[10] J. Chen, Z. Li, S. Yue, and Q. Gong, "Hybrid long-range surface plasmon-polariton modes with tight field confinement guided by asymmetrical waveguides," *Opt. Express*, vol. 17, no. 26, pp. 23 603–23 609, Dec. 2009.
[11] W. Xue, Y. Guo, and W. Zhang, "Modified surface plasmonic waveguide formed by nanometric parallel lines," *Chin. Phys. B*, vol. 19, no. 1, p. 017302, Jan. 2010.
[12] M. Ranjbaran and X. Li, "Performance-enhanced superluminescent diode with surface plasmon waveguide," *Opt. Express*, vol. 17, no. 26, pp. 23 643–23 654, Dec. 2009.
[13] V. Popescu, "Power absorption efficiency in plasmon—Polariton optical superconducting planar and rib waveguides," *Optoelectron. Adv. Mater. Rapid Commun.*, vol. 3, pp. 1259–1263, 2009.
[14] C. Reinhardt, A. Seidel, A. Evlyukhin, W. Cheng, and B. Chichkov, "Mode-selective excitation of laser-written dielectric-loaded surface plasmon polariton waveguides," *J. Opt. Soc. Amer. B, Opt. Phys.*, vol. 26, no. 12, pp. B55–B60, Sep. 2009.
[15] H. Luo, Y. Li, H. Cui, and Y. Hong, "Dielectric-loaded surface plasmon-polariton nanowaveguides fabricated by two-photon polymerization," *Appl. Phys. A, Solids Surf.*, vol. 97, no. 3, pp. 709–712, Nov. 2009.
[16] J. Serbin, A. Ovsianikov, and B. Chichkov, "Fabrication of woodpile structures by two-photon polymerization and investigation of their optical properties," *Opt. Express*, vol. 12, no. 21, pp. 5221–5228, Oct. 2004.
[17] R. Kiyan, C. Reinhardt, S. Passinger, A. L. Stepanov, A. Hohenau, H. R. Krenn, and B. N. Chichkov, "Rapid prototyping of optical components for surface plasmon polaritons," *Opt. Express*, vol. 15, no. 7, pp. 4205–4215, Apr. 2007.
[18] A. B. Evlyukhin, S. I. Bozhevolnyi, A. L. Stepanov, R. Kiyan, C. Reinhardt, S. Passinger, and B. N. Chichkov, "Focusing and directing of surface plasmon polaritons by curved chains of nanoparticles," *Opt. Express*, vol. 15, no. 25, pp. 16 667–16 680, 2007.
[19] A. Seidel, C. Ohrt, S. Passinger, C. Reinhardt, R. Kiyan, and B. Chichkov, "Nanoimprinting of dielectric loaded surface-plasmon-polariton waveguides using masters fabricated by 2-photon polymerization technique," *J. Opt. Soc. Amer. B, Opt. Phys.*, vol. 26, no. 4, pp. 810–812, Mar. 2009.
[20] T. Holmgaard and S. Bozhevolnyi, "Theoretical analysis of dielectric-loaded surface plasmon-polariton waveguides," *Phys. Rev. B, Condens. Matter*, vol. 75, no. 24, p. 245 405, Jun. 2007.
[21] T. Holmgaard, S. Bozhevolnyi, L. Markey, and A. Dereux, "Dielectric-loaded surface plasmon-polariton waveguides at telecommunication wavelengths: Excitation and characterization," *Appl. Phys. Lett.*, vol. 92, no. 1, p. 011124, Jan. 2008.
[22] A. L. Stepanov, J. R. Krenn, H. Ditlbacher, A. Hohenau, A. Drezet, B. Steinberger, A. Leitner, and F. R. Aussenegg, "Dielectric optical elements for surface plasmons," *Opt. Lett.*, vol. 30, no. 8, pp. 893–895, Apr. 2005.
[23] J. Grandidier, G. des Francs, S. Massenot, A. Bouhelier, L. Markey, J. C. Weeber, C. Finot, and A. Dereux, "Gain-assisted propagation in a plasmonic waveguide at telecom wavelength," *Nano Lett.*, vol. 9, no. 8, pp. 2935–2939, Aug. 2009.
[24] X. Guo, M. Qiu, J. Bao, B. Wiley, Q. Yang, X. Zhang, Y. Ma, H. Yu, and L. Tong, "Direct coupling of plasmonic and photonic nanowires for hybrid nanophotonic components and circuits," *Nano Lett.*, vol. 9, no. 12, pp. 4515–4519, Dec. 2009.
[25] T. Holmgaard, Z. Chen, S. I. Bozhevolnyi, L. Markey, and A. Dereux, "Dielectric-loaded plasmonic waveguide-ring resonators," *Opt. Express*, vol. 17, no. 4, pp. 2968–2975, Feb. 2009.
[26] T. Holmgaard, Z. Chen, S. I. Bozhevolnyi, L. Markey, and A. Dereux, "Design and characterization of dielectric-loaded plasmonic directional couplers," *J. Lightwave Technol.*, vol. 27, no. 24, pp. 5521–5528, Dec. 2009.